J|A|C|S
ARTICLES

Published on Web 07/27/2010

Six Different Assemblies from One Building Block: Two-Dimensional Crystallization of an Amide Amphiphile

Seokhoon Ahn and Adam J. Matzger*

Department of Chemistry and the Macromolecular Science and Engineering Program, University of Michigan, Ann Arbor, Michigan 48109-1055

Received June 9, 2010; E-mail: matzger@umich.edu

Abstract: A C_s-symmetric amide amphiphile containing a C_{18} alkyl chain exists in at least six crystalline phases at the liquid/solid interface; several of these phases display regularly arranged nanoscopic voids. Structural analysis of each phase reveals that highly symmetric and/or complex patterns arise through adopting various aggregates via noncovalent interactions, several of which are mediated by the unique hydrogen-bonding properties of the primary amide. The formation of each phase is interpreted in the context of the kinetic and thermodynamic behaviors, with some phases showing concentration-dependent stabilities, while others are purely kinetic in origin. This investigation contributes to understanding the factors that give rise to solid form diversity in two- and three-dimensional crystallization.

Introduction

Polymorphism is defined as the ability of a compound to exist in multiple crystalline phases, each differing solely in arrangement or conformation of molecules within a solid. Predicting the occurrence of this phenomenon in three-dimensional (3D) crystallization represents one of the greatest scientific challenges in solid-state chemistry. Furthermore, because of its importance in determining technologically relevant properties of a wide range of materials, including pharmaceuticals,[1,2] explosives,[3,4] and nonlinear optical materials,[5,6] there is significant financial motivation to generate a more predictive understanding of crystal polymorphism. One of the methods to study this phenomenon is the use of models such as two-dimensional (2D) crystals spontaneously formed at the liquid/solid interface; the reduced dimensionality of assembly dramatically simplifies the system with only 17 plane groups possible in 2D crystallization as compared to 230 space groups in 3D crystallization. Furthermore, the physisorbed molecular assemblies can be investigated with the aid of scanning tunneling microscopy (STM), offering submolecular resolution of both periodic and nonperiodic packing in a time-dependent fashion.[7−10] However, developing a compound showing the ability to exist in multiple phases in 2D crystallization is essential to study polymorphic phenomenon (e.g., the formation of a metastable polymorph during cocrystallization).[11−13] Here, we report the ability of a simple amide amphiphile with C_s symmetry to form at least six phases differing considerably in aggregation mode;[14] this level of phase diversity compares favorably to highly polymorphic molecules found in the Cambridge Structural Database (CSD) where only one compound, 5-methyl-2-[(2-nitrophenyl)amino]-3-thiophenecarbonitrile (ROY), exceeds five crystal structures.[15,16] The observation of highly symmetric and complex assemblies from this simple molecule provides an unprecedented view of the range of structural diversity that can arise from even a simple molecular building block.

Various tools to generate polymorphs in 3D such as controlling solvent/temperature,[17] epitaxial crystal growth/pseudoseeding,[18−23] polymer-induced heteronucleation,[24] and

(1) López-Mejías, V.; Kampf, J. W.; Matzger, A. J. *J. Am. Chem. Soc.* **2009**, *131*, 4554–4555.
(2) Vishweshwar, P.; McMahon, J. A.; Oliveira, M.; Peterson, M. L.; Zaworotko, M. J. *J. Am. Chem. Soc.* **2005**, *127*, 16802–16803.
(3) Vrcelj, R. M.; Sherwood, J. N.; Kennedy, A. R.; Gallagher, H. G.; Gelbrich, T. *Cryst. Growth Des.* **2003**, *3*, 1027–1032.
(4) van der Heijden, A.; Bouma, R. H. B. *Cryst. Growth Des.* **2004**, *4*, 999–1007.
(5) Nalwa, H. S.; Saito, T.; Kakuta, A.; Iwayanagi, T. *J. Phys. Chem.* **1993**, *97*, 10515–10517.
(6) Kwon, O. P.; Jazbinsek, M.; Yun, H.; Seo, J. I.; Kim, E. M.; Lee, Y. S.; Gunter, P. *Cryst. Growth Des.* **2008**, *8*, 4021–4025.
(7) Li, S. S.; Yan, H. J.; Wan, L. J.; Yang, H. B.; Northrop, B. H.; Stang, P. J. *J. Am. Chem. Soc.* **2007**, *129*, 9268–9269.
(8) Zhou, H.; Dang, H.; Yi, J. H.; Nanci, A.; Rochefort, A.; Wuest, J. D. *J. Am. Chem. Soc.* **2007**, *129*, 13774–13775.
(9) Scherer, L. J.; Merz, L.; Constable, E. C.; Housecroft, C. E.; Neuburger, M.; Hermann, B. A. *J. Am. Chem. Soc.* **2005**, *127*, 4033–4041.
(10) Fang, H. B.; Giancarlo, L. C.; Flynn, G. W. *J. Phys. Chem. B* **1999**, *103*, 5712–5715.
(11) Day, G. M.; Trask, A. V.; Motherwell, W. D. S.; Jones, W. *Chem. Commun.* **2006**, 54–56.
(12) Rafilovich, M.; Bernstein, J. *J. Am. Chem. Soc.* **2006**, *128*, 12185–12191.
(13) Lou, B. Y.; Bostroem, D.; Velaga, S. P. *Cryst. Growth Des.* **2009**, *9*, 1254–1257.
(14) The Two-Dimensional Structural Database (2DSD), a catalog of two-dimensional crystals formed at liquid/solid interfaces, reveals there is no compound showing ability to exist in over five different phases: Plass, K. E.; Grzesiak, A. L.; Matzger, A. J. *Acc. Chem. Res.* **2007**, *40*, 287–293.
(15) Chen, S.; Guzei, I. A.; Yu, L. *J. Am. Chem. Soc.* **2005**, *127*, 9881–9885.
(16) Nangia, A. In *Models, Mysteries, and Magic of Molecules*; Boeyens, J. C. A., Ogilvie, J. F., Eds.; Springer: Dordrecht, 2008; pp 63−86.
(17) Rodríguez-Spong, B.; Price, C. P.; Jayasankar, A.; Matzger, A. J.; Rodríguez-Hornedo, N. *Adv. Drug Delivery Rev.* **2004**, *56*, 241–274.
(18) Mitchell, C. A.; Yu, L.; Ward, M. D. *J. Am. Chem. Soc.* **2001**, *123*, 10830–10839.
(19) Hiremath, R.; Basile, J. A.; Varney, S. W.; Swift, J. A. *J. Am. Chem. Soc.* **2005**, *127*, 18321–18327.
(20) Hiremath, R.; Varney, S. W.; Swift, J. A. *Chem. Commun.* **2004**, 2676–2677.
(21) Friščić, T.; MacGillivrary, L. R. *Chem. Commun.* **2009**, 773–775.

10.1021/ja105039s

tailor-made additives[25−27] have found wide application. In 2D crystallization, additional packing motifs are typically obtained by controlling solvent identity.[28−33] For example, trimesic acid (TMA) forms chickenwire and flower phases depending on the alkyl-chain length of alkanoic acid solvents.[31] Recently, the role of concentration has been exploited to generate 2D nanoporous networks. For example, triangle-shaped fused dehydrobenzo[12]annulenes (DBA) bearing alkyl chains with 14 or 16 carbons form two different nanoporous structures arising from the close-packed structure by dilution, an effect demonstrated to be thermodynamically driven.[34] These examples reveal that, as in three dimensions,[35] the geometry of the building block plays a key role in determining arrangements in 2D crystallization; the molecular symmetry of TMA and triangle-shaped DBA derivatives facilitates the formation of high symmetry monolayers bearing 3-fold rotation axes, coinciding with molecular symmetry elements, through hydrogen-bonding or van der Waals interactions. In contrast with these high symmetry molecules, it has been shown that low symmetry amide amphiphiles can overcome the geometric barrier to build highly symmetric monolayers by forming an aggregate consisting of three molecules.[36] Here, we report several new phases of a low symmetry amide amphiphile bearing an alkyl chain including the unprecedented finding of six different phases: three close-packed structures and three nanoporous structures. In these structures, various numbers of inequivalent molecules in the asymmetric unit (e.g., $Z' = 2$, 3, and 6) were observed. These results are interpreted in the context of kinetic and thermodynamic concentration-dependent behavior under ambient conditions. These unique behaviors in 2D crystallization make it possible to distinguish the results from true polymorphism in 3D crystallization because concentration-dependent changes in stability cannot occur in 3D.

Results and Discussion

The molecular structure investigated here and models for selected aggregation modes are shown in Chart 1. **18-Amide** consists of hydrophobic and hydrophilic portions, and this amphiphilic nature plays a significant role in determining 2D crystal structure. The key interactions are (1) van der Waals interactions, which occur mainly among alkyl chains, and (2) hydrogen bonding between amide groups. These noncovalent interactions are satisfied to different extents in the various aggregates in Chart 1, and, if stable, each is expected to generate a different pattern at the liquid/highly oriented pyrolytic graphite (HOPG) interface. To investigate this possibility, solvents and concentration of **18-Amide** solutions were varied in the search for new phases much in the same manner as crystalline polymorph screening is carried out for three-dimensional crystals. Two different solvents, heptanoic acid and phenyloctane, were selected to vary polarity and induce different ordering of adsorbates because molecule−molecule, molecule−substrate, molecule−solvent, and solvent−substrate interactions conspire to determine the packing motif.

Chart 1. Molecular Structure of **18-Amide** and Aggregation Modes Experimentally Observed

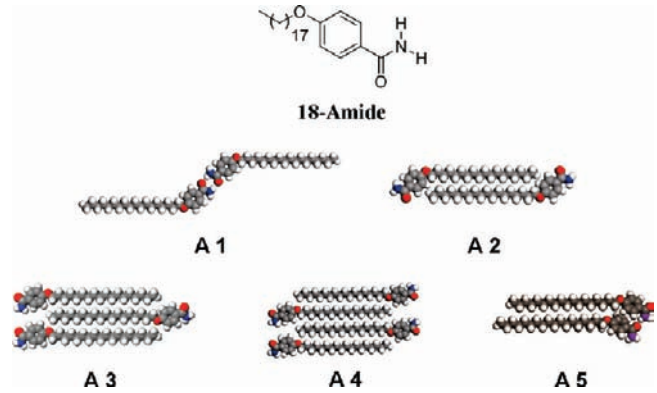

All phases of **18-Amide** formed at the liquid/HOPG interface are schematically shown in Figure 1. The number of molecules in the asymmetric unit (Z' value) is indicated for all phases except phase III, which has a one-dimensional (1D) periodicity resulting in an unusual unit cell with one infinite axis.[37] The amide amphiphile formed six different phases: three close-packed structures, one porous network with less than 1 nm voids, and two nanoporous networks with over 1 nm voids. Their unit cell parameters are shown in Table 1, and densities are calculated to discuss their stability in the context of thermodynamics. To describe each phase, aggregate modes observed from each phase are assigned to building blocks consisting of several **18-Amide** molecules as shown in Chart 1.

Close-Packed Structures. The close-packed structures of **18-Amide** are shown in Figure 2. One structure arises in 1.0 mM heptanoic acid solution (phase I), and two structures (phases II and III) arise in 0.10 mM phenyloctane solution. In recent studies, the application of Fourier transform infrared-attenuated total reflection (FTIR-ATR) revealed a direct relationship between aggregates in solution and hydrogen-bonded motifs in the crystal forms.[38] For example, hydrogen-bonded dimers were observed in chloroform solution of tetrolic acid, and this solution nucleated the α-form, whereas dimer formation was disturbed in ethanol solution, resulting in nucleating the β-form. The same considerations apply in the present case; in the phenyloctane solution of **18-Amide**, hydrogen-bonded dimers (**A1** mode)

(22) Braga, D.; Cojazzi, G.; Paolucci, D.; Grepioni, F. *CrystEngComm* **2001**, *38*, 1–3.
(23) Miura, H.; Ushio, T.; Nagai, K.; Fujimoto, D.; Lepp, Z.; Takahashi, H.; Tamura, R. *Cryst. Growth Des.* **2003**, *3*, 959–965.
(24) Price, C. P.; Grzesiak, A. L.; Matzger, A. J. *J. Am. Chem. Soc.* **2005**, *127*, 5512–5517.
(25) Weissbuch, I.; Addadi, L.; Lahav, M.; Leiserowitz, L. *Science* **1991**, *253*, 637–645.
(26) Thallapally, P. K.; Jetti, R. K. R.; Katz, A. K.; Carrell, H. L.; Singh, K.; Lahiri, K.; Kotha, S.; Boese, R.; Desiraju, G. R. *Angew. Chem., Int. Ed.* **2004**, *43*, 1149–1155.
(27) He, X. R.; Stowell, J. G.; Morris, K. R.; Pfeiffer, R. R.; Li, H.; Stahly, G. P.; Byrn, S. R. *Cryst. Growth Des.* **2001**, *1*, 305–312.
(28) Venkataraman, B.; Breen, J. J.; Flynn, G. W. *J. Phys. Chem.* **1995**, *99*, 6608–6619.
(29) Tahara, K.; Furukawa, S.; Uji-I, H.; Uchino, T.; Ichikawa, T.; Zhang, J.; Mamdouh, W.; Sonoda, M.; De Schryver, F. C.; De Feyter, S.; Tobe, Y. *J. Am. Chem. Soc.* **2006**, *128*, 16613–16625.
(30) Gutzler, R.; Lappe, S.; Mahata, K.; Schmittel, M.; Heckl, W. M.; Lackinger, M. *Chem. Commun.* **2009**, 680–682.
(31) Lackinger, M.; Griessl, S.; Heckl, W. A.; Hietschold, M.; Flynn, G. W. *Langmuir* **2005**, *21*, 4984–4988.
(32) Mamdouh, W.; Uji-i, H.; Ladislaw, J. S.; Dulcey, A. E.; Percec, V.; De Schryver, F. C.; De Feyter, S. *J. Am. Chem. Soc.* **2006**, *128*, 317–325.
(33) Li, Y. B.; Ma, Z.; Qi, G. C.; Yang, Y. L.; Zeng, Q. D.; Fan, X. L.; Wang, C.; Huang, W. *J. Phys. Chem. C* **2008**, *112*, 8649–8653.
(34) Lei, S. B.; Tahara, K.; De Schryver, F. C.; Van der Auweraer, M.; Tobe, Y.; De Feyter, S. *Angew. Chem., Int. Ed.* **2008**, *47*, 2964–2968.
(35) Brock, C. P.; Dunitz, J. D. *Chem. Mater.* **1994**, *6*, 1118–1127.
(36) Ahn, S.; Morrison, C. N.; Matzger, A. J. *J. Am. Chem. Soc.* **2009**, *131*, 7946–7947.
(37) Ahn, S.; Matzger, A. J. *J. Am. Chem. Soc.* **2009**, *131*, 13826–13832.
(38) Parveen, S.; Davey, R. J.; Dent, G.; Pritchard, R. G. *Chem. Commun.* **2005**, 1531–1533.

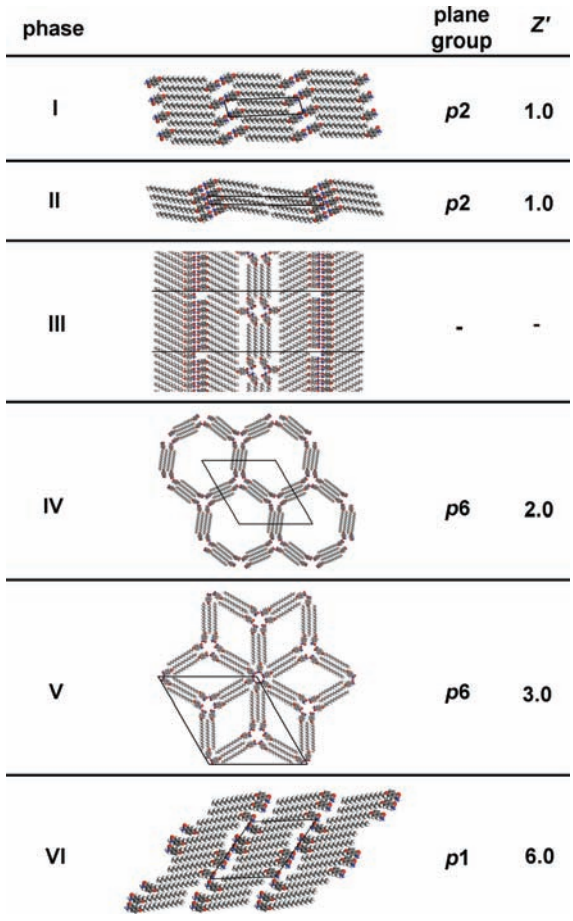

Figure 1. Schematic representation of all phases observed in 2D crystals of **18-Amide** with unit cells. The numbers of molecules in the asymmetric unit (Z' values) are indicated.

would be favored and nucleate to form phase II, which has the hydrogen-bonding network (phase II, Figure 5) without interdigitation of alkyl chains. On the other hand, in a heptanoic acid solution of **18-Amide**, the **A2** mode forms instead, resulting in the interdigitation of alkyl chains. The stabilites of these two phases are discussed below in the context of thermodynamics. For these two phases, each of the **18-Amide** molecules ($Z' = 1.0$) is related by a 2-fold rotation axis, resulting in *p*2 symmetry.

In 0.10 mM phenyloctane solution, another orientation (phase III, Figure 2c and d) was observed as a minor phase (see the Supporting Information). In this phase, there are two key structural characteristics: (1) the one-dimensionally periodic ordering, creating an infinite unit cell parameter along one axis (phase III, Figure 1), and (2) the coexistence of two different aggregation modes (**A1** and **A4**). Figure 2c and d clearly shows the molecular ordering of this phase. Aggregates consisting of four molecules (**A4**, Chart 1) are ordered along one axis between two columns of the sort comprising phase II. Because it is not feasible to form appropriate hydrogen bonds between **A4** aggregates in this arrangement, additional molecules are required to stabilize this phase by hydrogen bonding. The proposed model is shown in Figure 2d. This model is supported by the vacancies of periodically ordered aromatic rings in the phase II-type columns indicated by blue arrows (Figure 2c). Although the aromatic rings are absent, the missing alkyl chains are not observed, indicating the opposite orientation of **18-Amide**. These molecules play a critical role in promoting compatibility between two different aggregation modes by hydrogen bonding with **A4** aggregates inserted between the columns resembling phase II. This phase demonstrates that if there is compatibility of geometry and functionality between the different aggregates, more complex nanoscale features can arise.

Porous Network (<1 nm Voids). Recently, it has been reported that nanoporous networks with cavities are formed from dilute solution where the adsorption−desorption equilibrium determines the surface coverage of the close-packed versus nanoporous structure.[39−41] When the concentrations of the heptanoic acid solution were reduced from 1000 to 20 μM, a porous network with less than 1 nm voids was observed in the concentration range from 500 to 100 μM (phase VI, Figure 3). The high-resolution STM images of this phase reveal that there are six molecules with coexistence of both **A2** and **A5** aggregation modes in the unit cell. The combination of these different modes causes a periodic porous network with wavy boundaries between columns as shown in Figure 3. To maintain a network of hydrogen bonds at the column interfaces, the amide groups must all point in the same direction. Furthermore, the lack of contrast between adjacent columns suggests that amide orientation does not flip between columns.[42,43] Therefore, the plane group of this phase is *p*1, and the crystallographic asymmetric unit contains six molecules ($Z' = 6.0$); no examples of Z' equal to 6.0 are found in the 2DSD.[14]

Nanoporous Networks (>1 nm Voids). When the concentration of the analyte in phenyloctane solution was varied from 100 to 5 μM, two different nanoporous networks were observed in the concentration range from 33 to 5 μM: the rhombic nanoporous network (Figure 4c) and the honeycomb network (Figure 4a). The characteristics of the rhombic network formed by **18-Amide** analogues with shorter alkyl chains were previously reported.[36] From dilute solutions, **18-Amide** preferably forms the rhombic nanoporous network instead of forming a close-packed structure (phase II). **18-Amide** forms an aggregate of three molecules (**A3**, Chart 1) to generate 3- and 6-fold rotation axes in the monolayer symmetry of *p*6 (Figure 4d). This **A3** aggregate corresponds to the number of molecules in the asymmetric unit ($Z' = 3.0$). A search of the 2DSD reveals that this high value is very uncommon, occurring in 0.6% of entries where most crystals (over 86%) in 2D and 3D have $Z' = 1.0$ or 0.5.[14,44] The $Z' = 3.0$ indicates that three molecules are related to all others by 3- and 2-fold rotation axes, giving *p*6 symmetry. Because **A3** mode is not kinetically preferable in phenyloctane, the formation of phase V is due to the influence of thermodynamic factors leading to forming less dense forms in dilute solutions. This claim is supported by the observation of the phase transformation from phase II to phase V in two different situations: (1) when 10 μM solution was placed on HOPG, phase II was initially observed as a kinetic form and subsequently transformed to phase V within 1 h; and (2) when the concentration of the solution on HOPG was decreased by adding solvent from 50 to 20 μM, the phase transformation from

(39) Tahara, K.; Lei, S.; Mossinger, D.; Kozuma, H.; Inukai, K.; Van der Auweraer, M.; De Schryver, F. C.; Hoger, S.; Tobe, Y.; De Feyter, S. *Chem. Commun.* **2008**, 3897–3899.
(40) Kampschulte, L.; Werblowsky, T. L.; Kishore, R. S. K.; Schmittel, M.; Heckl, W. M.; Lackinger, M. *J. Am. Chem. Soc.* **2008**, *130*, 8502–8507.
(41) Tahara, K.; Okuhata, S.; Adisoejoso, J.; Lei, S.; Fujita, T.; De Feyter, S.; Tobe, Y. *J. Am. Chem. Soc.* **2009**, *131*, 17583–17590.
(42) Plass, K. E.; Kim, K.; Matzger, A. J. *J. Am. Chem. Soc.* **2004**, *126*, 9042–9053.
(43) De Feyter, S.; Grim, P. C. M.; van Esch, J.; Kellogg, R. M.; Feringa, B. L.; De Schryver, F. C. *J. Phys. Chem. B* **1998**, *102*, 8981–8987.
(44) Steiner, T. *Acta Crystallogr., Sect. B* **2000**, *56*, 673–676.

Table 1. Experimental and Computed Unit Cell Parameters for All Two-Dimensionally Ordered Phases Observed for **18-Amide**

	computed			experimental			
phase	*a* (Å)	*b* (Å)	α (deg)	*a* (Å)	*b* (Å)	α (deg)	density (Da/nm^2)
I	37.8	9.15	101	38.3 ± 0.3	9.8 ± 0.3	102 ± 2	229.5
II	63.1	5.1	111	67.8 ± 1.1	5.1 ± 0.1	117 ± 1	259.4
IV	78.5	78.3	120	77.2 ± 1.9	77.0 ± 2.0	120 ± 1	86.0
V	77.5	77.5	120	80.1 ± 0.4	80.0 ± 0.4	120 ± 1	134.8
VI	34.8	37.6	126	37.4 ± 2.0	40.0 ± 2.0	128 ± 2	220.8

phase II to phase V was observed. The driving force for this transformation is discussed below in the context of thermodynamics. In addition, the present case demonstrates that the size of the rhombic shaped void is controllable by adjusting alkyl chain length because the void width of 2.6 × 5.3 nm^2 is enlarged from the 2.2 × 4.0 nm^2 formed by the amide amphiphile containing a C_{12} alkyl chain.[36]

During modeling of the rhombic network (phase V), the aggregation mode of **A4** was considered, and it was revealed that **A4** can generate only 3-fold rotation axes potentially leading to a honeycomb network. This honeycomb network (phase IV) with a void diameter of 6.3 nm was observed in dilute phenyloctane solutions. This phase has not been observed as a major phase at all ranges of concentrations investigated and was observed as an intermediate form during the phase transformation from phase II to phase V. The formation of phase IV during this phase transformation is discussed below in the context of thermodynamics. To satisfy the monolayer symmetry of *p*6 (Figure 4a), an aggregate must consist of four molecules (**A4**, Chart 1) to generate exclusively 3-fold rotation axes simultaneously by hydrogen bonding at two different positions in a unit cell (Figure 4b). In this case, the crystallographic asymmetric unit is two ($Z' = 2.0$). Two molecules are related with 3-fold rotation axes and a 2-fold rotation axis, giving rise to *p*6 symmetry. The appearance of Z' equal to 2.0 is also notable for its rarity (6.3% in 2DSD).[14]

Hydrogen-Bonding Motifs. The computed models for all phases provide the hydrogen-bonding structures shown in Figure 5. Hydrogen bonding between amide groups plays a key role in creating complex features because all phases have different motifs. Phases I and II both contain amide dimers with local centers of symmetry; however, in phase I these dimers are well separated due to the interdigitation of alkyl chains (phase I, Figure 5), whereas in phase II a continuous column of amides connected by additional hydrogen bonding is present (phase II, Figure 5). Although both phases could arise from **A1** aggregates, only phase I can form from **A2** aggregates due to solvation in heptanoic acid (phase II, Figure 5). For phase III, two **18-Amide**

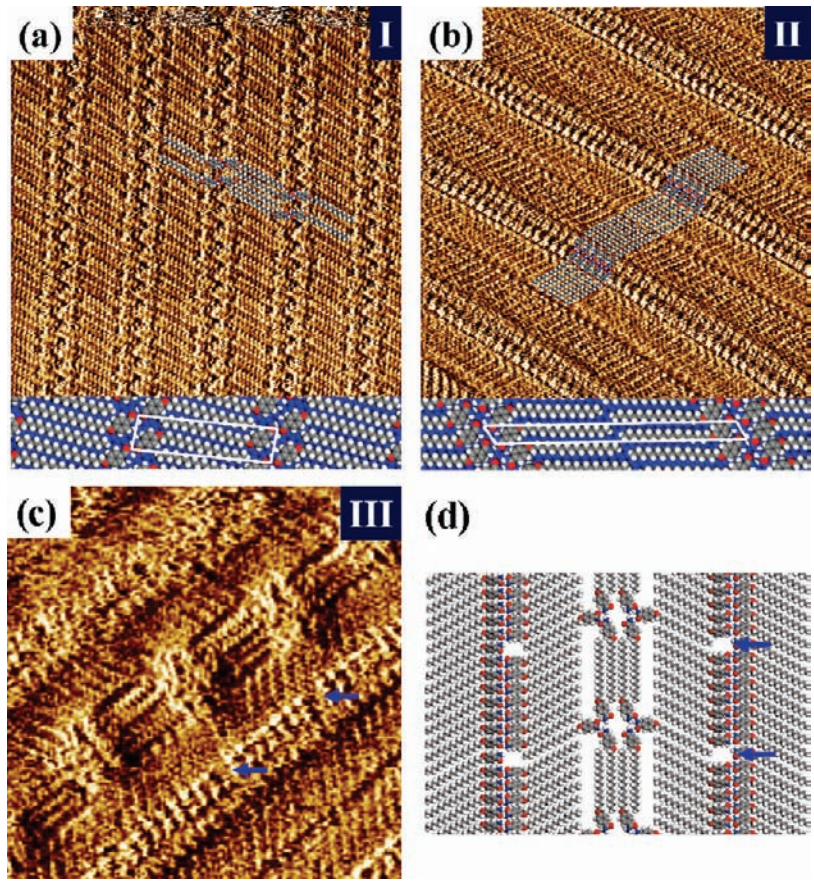

Figure 2. Three different close-packed structures of **18-Amide** formed at the liquid/HOPG interface. (a) STM image (20 × 20 nm^2) and the computed model of the monolayer in 1.0 mM heptanoic acid solution. (b) STM image (20 × 20 nm^2) and the computed model of the major phase in 100 μM phenyloctane solution. (c) STM image (15 × 15 nm^2) and (d) the computed model of a minor phase in 100 μM phenyloctane solution. The computed models are superimposed on STM images. Blue arrows indicate vacancies in the columnar packing.

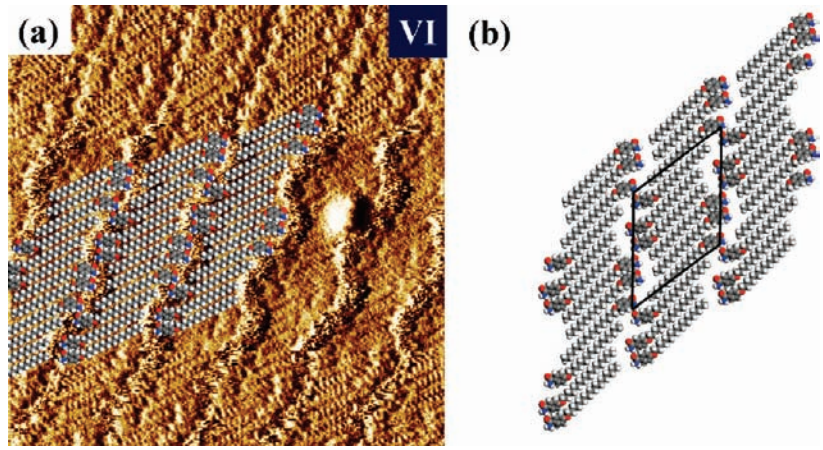

Figure 3. The porous structure from dilute heptanoic acid solutions: (a) STM image (20 × 20 nm^2) obtained from 500 μM solution and (b) the computed model of phase VI. The wavy boundaries between columns in the STM image originate from the void space of phase VI.

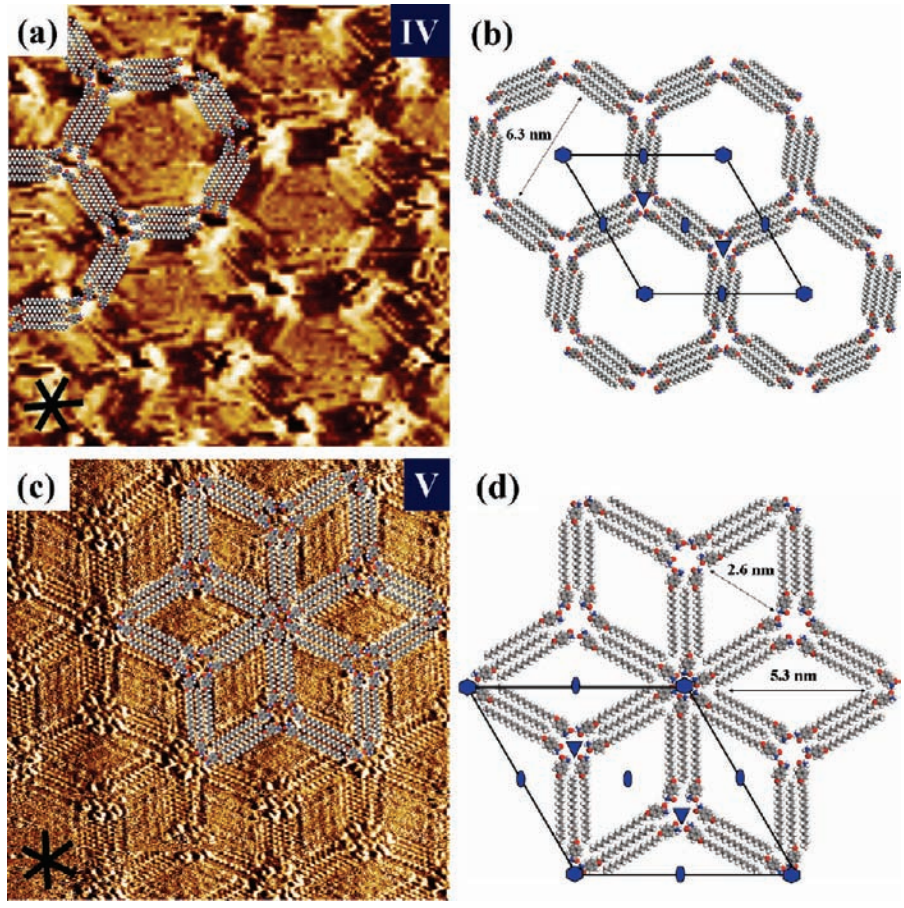

Figure 4. Two different nanoporous structures from dilute phenyloctane solutions: (a) STM image (20 × 20 nm^2) and (b) the computed model of the honeycomb network from 33 μM phenyloctane solution; (c) STM image (20 × 20 nm^2) and (d) the computed model of the rhombic nanoporous network from 25 μM phenyloctane solution. The black axes indicate the main symmetry of HOPG under the monolayer. The computed models are superimposed on STM images.

molecules act as a connector between aggregates consisting of 4 molecules (phase III, Figure 5). For the rhombic nanoporous network (phase V), there are 3- and 6-fold rotation axes formed by the hydrogen-bonding network, whereas for the honeycomb network (phase IV), an aggregate of 4 molecules generates exclusively 3-fold rotation axes. For phase VI, the two different **A2** and **A5** modes are stabilized by forming hydrogen bonds as shown in Figure 5. The combination of these two modes causes a wave-like pattern of voids.

The observation of one-dimensional ordering (phase III) and high Z' values for three porous networks investigated here reveals that the simple amide amphiphile with C_s symmetry, which upon adsorption is unable to be coincident with any symmetry elements, has the ability to generate highly symmetric patterns by forming various aggregates using noncovalent interactions. The fact that all six phases have different hydrogen-bonding motifs reveals that hydrogen bonding plays a critical role in not only forming aggregates but also in their stabilization.

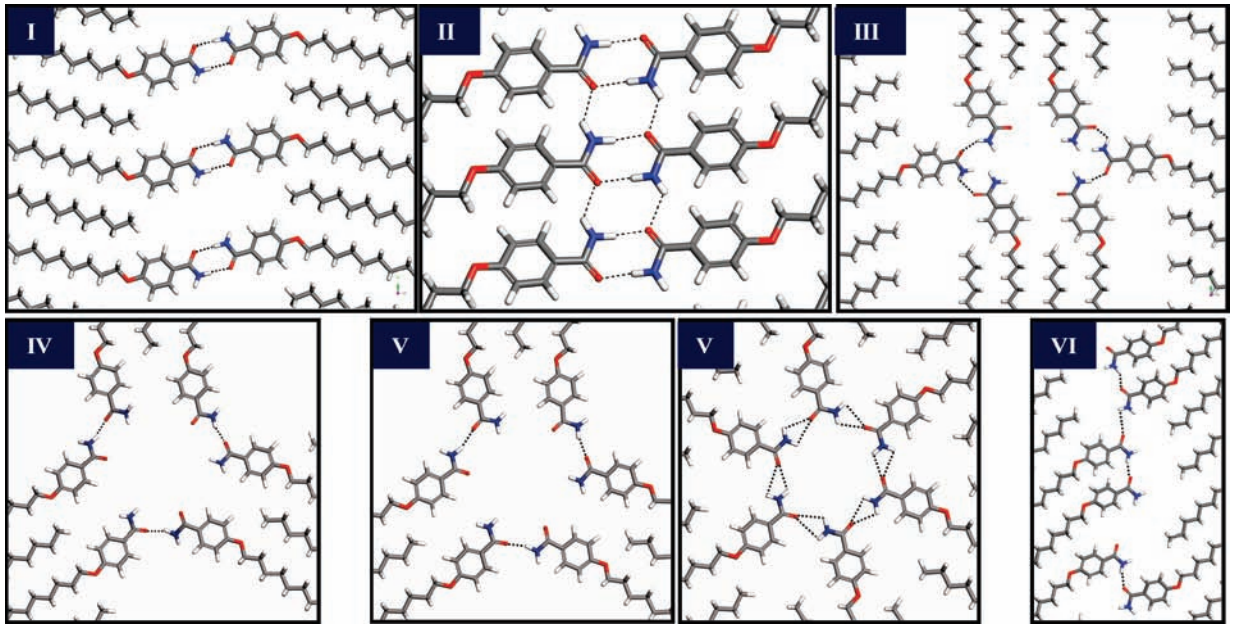

Figure 5. The hydrogen-bonding networks observed in six phases. Hydrogen bonds are indicated by a dotted line. Phase V has two different networks to generate 3- and 6-fold rotation axes.

Table 2. Lattice Energies of All Two-Dimensionally Ordered Phases of **18-Amide** Computed by the COMPASS Force Field (kcal/mol)[a]

phase	I	II	IV	V	VI
lattice energy	–17.5	–23.0	–12.1	–12.3	–15.8
van der Waals term	–12.3	–13.6	–9.4	–9.0	–12.1
electrostatic term	–5.2	–9.4	–2.7	–3.3	–3.7

[a] These values represent the energy obtained by the formation of the 2D crystals from isolated **18-Amide** molecules.

This is the key to forming high symmetry or complex nanoscale features with high Z' using a low symmetry amide amphiphile. This finding has an analogy with trends in three-dimensional crystals, where $Z' > 1$ has been associated with strong noncovalent interactions.[42,45] In the present case, dilution also greatly contributes to stabilizing less dense forms through a thermodynamic mechanism.[34]

Thermodynamics. Molecular mechanics is a complementary tool to STM that provides not only structural information at the atomic level, sometimes obscured in the experimental images, but also thermodynamic information providing the relative stabilities of phases.[46] In the two most dense phases, the hydrogen bonding in phase II more significantly contributes to stabilizing the phase than in phase I based on evaluation of the electrostatic term (Table 2) and contributes to the overall greater predicted stability of phase II. However, a transformation from phase II to I was observed when adding heptanoic acid solution to the phenyloctane solution. In contrast, no phase transformation from phase I to II was observed by adding phenyloctane solution to the heptanoic acid solution. This result indicates that phase I is more stable than phase II. However, phase transformation from phase II to I in the homogeneous phenyloctane solution has not been observed within several hours. The plausible explanation for this is that the formation of a non-hydrogen-bonded aggregate before adsorption in phenyloctane requires overcoming a large energy barrier to transform to phase I. This experiment reveals that the substrate and solvent, which can affect adsorption energy of solutes and the solute−surface interaction,[28] also play a key role in stabilization of phases where the effects of the graphite substrate and solvent molecules are difficult to incorporate in the modeling.[47]

Consistent with the low densities of phases IV and V, the lattice energies are much more positive than the close-packed structures. Phase VI is less stable than the close-packed structures and much more stable than the other nanoporous structures. For phase VI, the density is about 9 Da/nm^2 smaller than that of phase I (229.5 Da/nm^2), and much higher than that of phases IV (86.0 Da/nm^2) and V (134.8 Da/nm^2) due primarily to smaller void size.[48] The computed model of phase VI indicates that the stabilization from electrostatic term of phase VI is smaller by 1.5 kcal/mol than that of phase I due to a relatively low extent of hydrogen bonding. For the other nanoporous networks, phase V is more stable than phase IV by about 0.2 kcal/mol. Phase V is more stabilized by hydrogen bonding due to a relatively favorable arrangement around the 6-fold rotation axis (phase V, Figure 5) where such a hydrogen-bonding network is not present in phase IV. Phase IV is more stabilized by van der Waals interaction due to the formation of an aggregate consisting of four molecules as compared to the three molecules in phase V; in both cases, close packing is only satisfied within the aggregate, and therefore a smaller aggregate has a greater percentage of alkyl chains lacking full van der Waals contact. For these competing reasons, phases IV and V

(45) Anderson, K. M.; Goeta, A. E.; Hancock, K. S. B.; Steed, J. W. *Chem. Commun.* **2006**, 2722–2722.

(46) Phase III was not considered to compare stabilities of phases due to the one-dimensional ordering, which makes construction of a unique model impossible.

(47) The doubly periodic and noncommensurate relationship between the substrate and overlayer prohibits constructing the periodic model with substrate. In addition, solvent−molecule interactions with fully periodic 2D crystals are not feasible using experimental data because the solvent molecules are too fleeting to allow STM imaging.

(48) The densities were obtained by multiplication of the molecular weight (Da) by the number of molecules in the unit cell, followed by division by the surface area in square nanometers (nm^2).

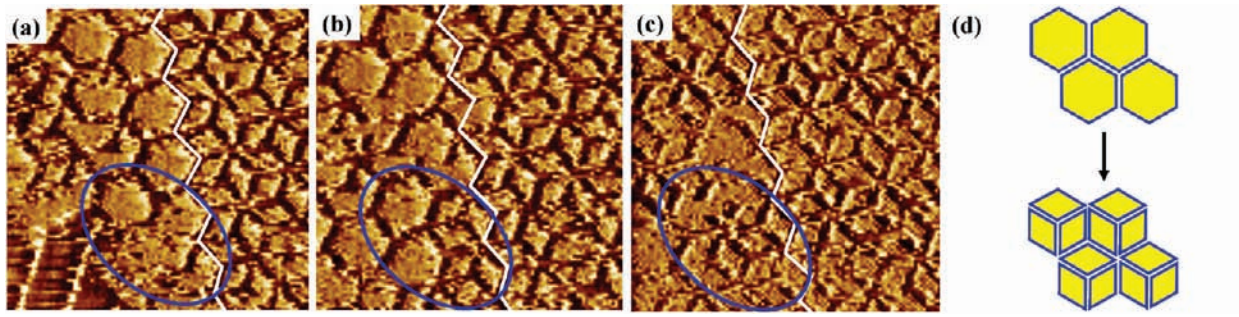

Figure 6. Sequential STM images (40×40 nm^2) obtained from a 33 μM **18-Amide** in phenyloctane solution on HOPG. These images clearly show the phase transformation from phase II to phase V where phase IV was observed as an intermediate. (a) Coexistence of phases II, IV, and V was observed ($t = 0$), and a white zigzag line is designated to distinguish phases IV and V. (b) After 100 s, phase II transforms to phase IV, and some of the hexagonal pores transform to the rhombic pore (blue oval). (c) After 250 s, phase IV transforms to phase V. (d) Schematic illustration of the transformation from the hexagonal pore to the rhombic pore observed in the blue oval.

have similar lattice energies. However, the stabilization energy per unit area basis is a more appropriate measure of the relative stability of monolayers because only a fixed amount of surface area is available for monolayer formation.[49] The lattice energies are -4.3 kcal/nm^2 for phase V and -2.7 kcal/nm^2 for phase IV, indicating a greater stabilization for phase V due to higher density of noncovalent interactions. This molecular mechanics calculation supports that phase V is a more thermodynamically stable form than is phase IV, and indeed this is observed (vide infra). It must be noted that in cases where the concentration of adsorbate molecules is very low, a regime can be entered where insufficient molecules are available to cover the substrate completely. In such a case, molar adsorption energy rather than energy on a per unit area basis may determine structure.

Comparison of close-packed and nanoporous structures provides additional insight regarding phase selection in 2D crystallization. For example, transformation from phase II to phase V is observed as the concentration decreases. Phase II has twice the density and is more stable by 10.7 kcal/mol than phase V based on computation. This large stability difference may be overcome by three factors proposed by De Feyter, Tobe, and co-workers: (1) substrate effects such as epitaxial stabilization by HOPG, (2) solvent coadsorption in periodically ordered voids providing additional weak interactions with adsorbed molecules, and (3) equilibrium of adsorption−desorption in solution.[34,41] The symmetries of phases IV and V are well matched with the symmetry of HOPG, and furthermore mobile solvent molecules may exist in void space within 2D crystals, thereby dramatically reducing the energy difference between phase II and V. In addition, the newly formed equilibrium of adsorption−desorption by dilution can cause the phase transformation from the close-packed structure (phase II) to a less dense form (phase V). To experimentally verify whether or not phase V is a thermodynamic form, dilution of phenyloctane solution on HOPG was conducted. When 2.0 μL of the 50 μM solution was put on HOPG, the solution covered the entire HOPG surface (9×9 mm^2), and phase II was observed as a major phase. The sample solution was diluted by adding 1.0 μL phenyloctane aliquots to achieve a concentration of 20 μM while imaging the monolayer at each dilution step. At 33 μM, the phase transformation from phase II to phase V was observed, and phase IV was observed as an intermediate during this transformation (Figure 6). In Figure 6a, the coexistence of phases II, IV, and V is shown. After 100 s, phase II transformed to phase IV, and some of phase IV transformed to phase V (blue oval in Figure 6b). After 250 s, phases II and IV had completely transformed to phase V (Figure 6c). This result indicates that phase IV is an intermediate during the transformation to the thermodynamically stable form V under the newly formed equilibrium. Figure 6d shows a schematic illustration of symmetry change during the phase transformation observed in the blue oval. After desorption of phase II, the honeycomb network (phase IV) is formed because it is more kinetically favored than phase V, and then one hexagonal pore is divided into three rhombic pores by reorganization, resulting in forming the rhombic network (phase V). Because phase V exists as a thermodynamically stable form in dilute solutions, phase IV, which has 36.2% lower density than phase V, may be stabilized upon further dilution. Attempts to experimentally verify this possibility were not successful. Applying more dilute solutions led to the formation of phase V accompanied by disordered regions, suggesting that phase IV is only a kinetic form (see the Supporting Information).

Contrast to 3D Polymorphism. The observed behaviors regarding the phase transformation from phase II to phase V are similar to the phenomena of monotropy and enantiotropy in 3D polymorphism, where monotropy occurs when one polymorph is thermodynamically more stable than other polymorphs at all temperatures below melting and enantiotropy indicates that the relative thermodynamic stability of two forms reverses at some temperature. The present case shows analogous behavior of phase stability versus concentration rather than temperature (Figure 7) and can be described as a pycnotropism. Phases II and V show the enantiopycnotropic behavior because phase II transforms to phase V as the concentration decreases where coexistence with the mostly same surface coverage was observed at 33 μM (see the Supporting Information). Phase IV and phase V are monopycnotropic as shown in Figure 7b because phase V has been observed as an intermediate during the phase transformation and has not been observed as a thermodynamically stable form in all of the concentration range where 2D crystallization occurs. The Gibbs phase rule states that analogous thermodynamically driven phase transformations versus concentration cannot be observed in 3D polymorphism, whereas the phase transformation versus concentration is now being recognized as a general feature in 2D crystallization. This discrepancy can be understood by recognizing that 2D crystals have additional contributions to phase selection due to the existence of HOPG and solvent and the relative influence of these changes with concentration. This observation is actually

(49) Kim, K.; Plass, K. E.; Matzger, A. J. *J. Am. Chem. Soc.* **2005**, *127*, 4879–4887.

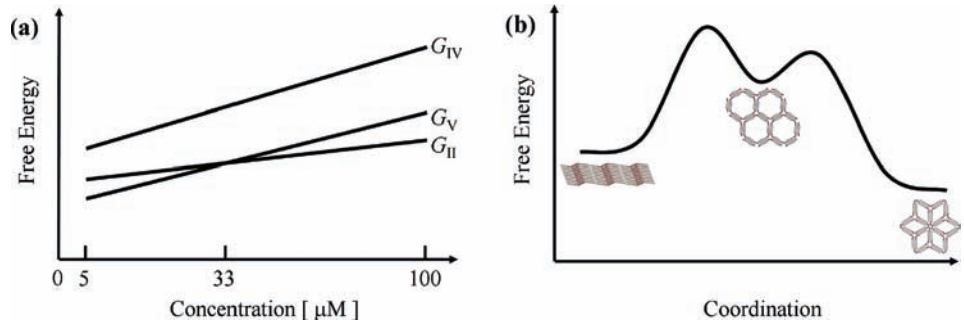

Figure 7. Schematic diagram of free energy versus concentration of phases II, IV, and V at a given temperature during two-dimensional crystallization: (a) schematic illustration of monopycnotropy and enantiopycnotropy for phases II, IV, and V of **18-Amide** and (b) reaction coordination diagram describing the phase transformation from phase II to phase V below 33 μM where phase IV is observed as an intermediate.

more similar to concentration-dependent formation of solvates in 3D crystallization and explains why alternative packing arrangements in two-dimensional crystallization should be termed pseudopolymorphs.

Conclusion

Studying the similarity and differences between two- and three-dimensional crystallization is essential to construct a bridge between them. This investigation demonstrates the ability of a simple amide amphiphile to exist in various ordered phases, even in the reduced dimensionality offered by adsorption to a surface, through adopting various aggregation modes. The combination of dilution and multiple hydrogen bonding motifs appears to favor the formation of $Z' > 1$, and there is analogy here to the suggestion that the absolute strength of noncovalent interactions can lead to forming $Z' > 1$ structures in three-dimensional crystallization. Furthermore, monopycnotropy and enantiopycnotropy are illuminated thermodynamic descriptors for the emergent phenomenon of concentration-dependent changes in thermodynamic phase stability, a phenomenon lacking analogy in polymorphic crystals. The particular system described presents challenges for theory to explain the energetic relationships among forms and how kinetic factors can give rise to phase selection within the context of such a simple molecule assembled on a surface. From an experimental standpoint, such rich phase diversity has not previously been achieved, and the design of molecules capable of adopting several energetically viable aggregation modes may be a model for future discovery efforts.

Acknowledgment. This work was supported by the National Science Foundation (CHE-0616487).

Supporting Information Available: Experimental details, additional STM images, and modeling of phases III and IV. This material is available free of charge via the Internet at http://pubs.acs.org.

JA105039S